Int. J. Electrochem. Sci., 11 **(2016)** 7830 – 7842, doi: 10.20964/2016.09.40

International Journal of ELECTROCHEMICAL SCIENCE
www.electrochemsci.org

Short Communication

Probability Analysis of Island Distribution at the Early Stage in Electrodeposition Based on a Fixed Length Segment Model

M. Saitou

Department of Mechanical Systems Engineering, University of the Ryukyus, 1 Senbaru Nishihara-cho Okinawa, 903-0213, Japan
E-mail: saitou@tec.u-ryukyu.ac.jp

Received: 7 June 2016 / *Accepted:* 11 July 2016 / *Published:* 7 August 2016

A fixed length segment model that describes a random distribution of segments that have a fixed number of sites at which islands can nucleate is proposed. The model is based on observations of several metal islands aligned without gaps on a curved line at the early stage in electrodeposition. The model has the advantage of being able to calculate analytically the number of two, three, and four islands aligned without gaps on the segment. In addition, the two-dimensional distribution of the segment derived analytically yields the limiting radius of the island beyond which the island cannot grow with time. The analytical results such as the expected value of the number of the two, three, and four islands and the limiting radius of the island are well consistent with the copper island distribution electrodeposited on an ITO glass at the early stage using a solution of *copper* (II) *sulfate* pentahydrate and potassium sodium tartrate. The characterization of the ITO glass surface as a nucleation site is demonstrated using the fixed length segment model.

Keywords: probability, fixed length segment model, islands aligned without gaps, segment distribution, limit radius, copper electrodeposition

1. INTRODUCTION

Nucleation and growth in electrodeposition have attracted many researchers owing to scientific and technological interests [1-11]. Phenomenological expressions for nucleation have been developed on the basis of the Avrami theorem [12-13]. Equations including the current density and growth time for two special cases called the progressive nucleation and instantaneous nucleation [6-7] are often used to determine which case is applicable to experimental results.

The Avrami theorem assumes random and homogeneous nucleation. In other words, any site on a substrate surface has an equal probability for nucleation. However, electrodeposits generated on the

substrate, which are called islands in this study, appear as if they were aligned on a curved line. Even if a glassy carbon substrate [14], highly ordered pyrolytic graphite (Hopg) substrate [15-16], and indium tin oxide (ITO) glass substrate [17], which have smooth surfaces at an atomic level, are used, the islands aligned on the curved line are observed by a scanning electron microscope (SEM), atomic force microscope (AFM), and laser confocal microscope. The heterogeneous growth of the island is two-dimensional at the early stage in electrodeposition. Here, the word, two-dimensional, means that no new island generation on the island takes place. The curved line indicates that nucleation sites exist side by side on the curved line. At the early stage in electrodeposition, two, three and four islands aligned without gaps are often observed. However, there have been very few studies that focus on the probability of the generation of islands aligned without gaps on the curved line. In the previous studies, every surface on a substrate was assumed to have the same nucleation sites.

We propose the model that the curved line is treated as a finite length segment that is randomly distributed on the substrate. This finite length segment model has the advantage that the probability for nucleation can be analytically derived using a Poisson distribution. In addition, the stochastic distribution of the segment can also be derived analytically using the Poisson distribution. According to the proposed model, the surface that has nucleation sites can be characterized by a new concept of the finite length segment introduced in this study, namely, the number of the finite length segment and its distribution on the surface. Hence, this study focuses not on the nucleation behaviour dependent on electrochemical parameters but on the characteristic of the surface as a nucleation site. As the distribution of the segment in two dimensions provides the distance between segments, the distribution of the segment yields the limiting radius of the island beyond which the island cannot grow [18].

In order to investigate a validity of the finite length segment model, copper electrodeposition on the ITO glass using a solution of *copper* (II) *sulfate* pentahydrate and potassium sodium tartrate is chosen because SEM images of the copper islands generated at the early stage show that the copper islands are two-dimensional and no overlap between the islands is observed. The expected value calculated analytically will be demonstrated to be well consistent with the experimental values in copper electrodeposition, and to characterize the surface of the ITO glass using the number of the finite length segment and the critical island size derived from the distribution of the finite length segment.

2. PROBABILITY ANALYSIS

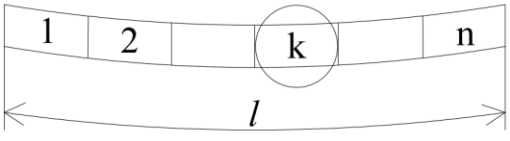

Figure 1. Schematic diagram of a finite length segment on which islands are generated. A probability for the generation of the island has the same at any sites. The circle shows an island generated at the kth site on the segment of length *l*.

Figure 1 shows a segment with a fixed length, *l* that is a curved segment and has n sites at which the island denoted by a circle nucleates. Each site has an equal probability to generate the island and independently generates the island. Let N_s and N_i be the number of segments and that of the island, the probability to generate m islands on the segment is given by the Poisson probability having the mean value $\lambda_0 = N_i/N_s$,

$$P_0^m = \frac{\lambda_0^m e^{-\lambda_0}}{m!}. \quad (1)$$

For simplicity, all the segments are assumed to have a fixed length *l*.

2.1 Probability that two islands are aligned without a gap on the segment

Let us consider the probability that two islands are aligned on adjacent sites as shown in Fig. 2.

(1) Case of Fig. 2 (a)

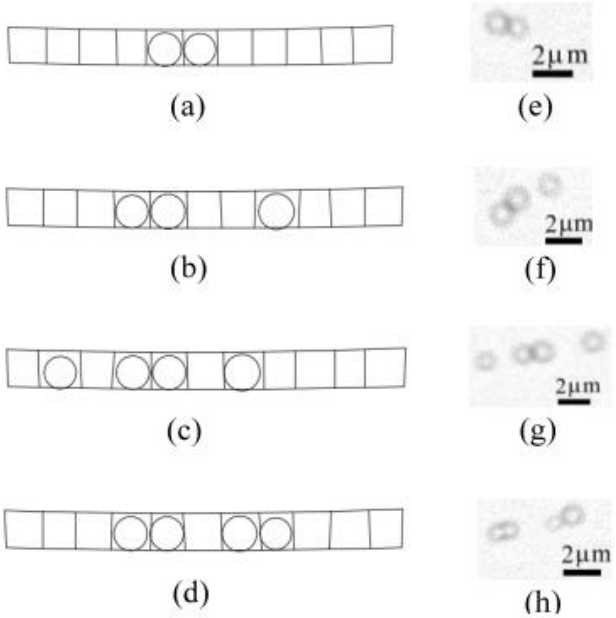

Figure 2. Schematic diagram from (a) to (d) of two islands aligned without a gap on a segment and corresponding SEM images from (e) to (h) of copper islands generated on the ITO glass.

When two islands are generated and the two islands are located in the adjacent sites, the probability is given by

$$P_0^2 \frac{(n-1)C_1}{nC_2} = \frac{\lambda_0^2 e^{-\lambda_0}}{n}. \quad (2)$$

The first and second term on the left-hand side indicate the probability that the two islands are generated on the segment and the probability that the two islands are located without a gap.

(2) Case of Fig. 2 (b)

When three islands are generated and only two islands among them are located in the adjacent sites, the probability is given by

$$\frac{(n-3)\lambda_0^3 e^{-\lambda_0}}{n(n-1)}. \quad (3)$$

(3) Case of Fig. 2 (c)

When four islands are generated and only two islands among them are located in adjacent sites, the probability is given by

$$\frac{(n-5)(n-4)\lambda_0^4 e^{-\lambda_0}}{2n(n-1)(n-2)}. \quad (4)$$

(4) Case of Fig. 2 (d)

When four islands are generated and two pairs are located separately, the probability is given by

$$\frac{(n-4)\lambda_0^4 e^{-\lambda_0}}{n(n-1)(n-2)}. \quad (5)$$

As the probability that other cases take place is very small, we can ignore them. Finally, the probability that the two islands are aligned without a gap on the segment is given by the summation of Eqs. (2), (3), (4), and (5).

2.2 Probability that three islands are aligned without gaps on the segment

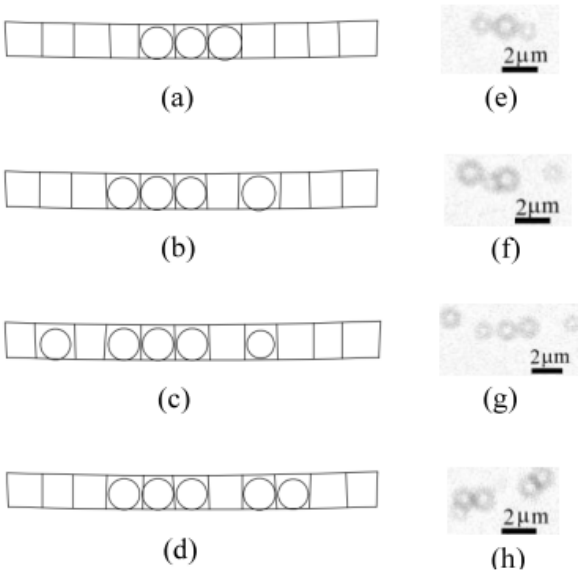

Figure 3. Schematic diagram from (a) to (d) of three islands aligned without gaps on a segment and corresponding SEM images from (e) to (h) of copper islands generated on the ITO glass.

Let us consider the probability that three islands are located without gaps as shown in Fig. 3.

(1) Case of Fig. 3 (a)

When three islands are generated and the three islands are located without gaps, the probability is given by

$$\frac{\lambda_0^3 e^{-\lambda_0}}{n(n-1)}. \quad (6)$$

(2) Case of Fig. 3 (b)

The four islands are generated and three islands among them are located without gaps. The remaining island is located far from the three islands. The probability is given by

$$\frac{(n-4)\lambda_0^4 e^{-\lambda_0}}{n(n-1)(n-2)}. \quad (7)$$

(3) Case of Fig. 3 (c)

Five islands are generated and three islands among them are located without gaps. The remaining islands are located far from each other on the segment. The probability is given by

$$\frac{(n-6)(n-5)\lambda_0^5 e^{-\lambda_0}}{2n(n-1)(n-2)}. \quad (8)$$

(4) Case of Fig. 3 (d)

Five islands are generated and are separated into two and three islands. The two and three islands are located without gaps. The probability is given by

$$\frac{(n-5)\lambda_0^5 e^{-\lambda_0}}{n(n-1)(n-2)(n-3)}. \quad (9)$$

As the probability that other cases take place is very small, we can ignore them. Finally, the probability that three islands are aligned without gaps on the segment is given by the summation of Eqs. (6), (7), (8), and (9).

2.3 Probability that four islands are alighted without gaps on the segment

When four islands are generated and the four islands are located without gaps on the segment, the probability is given by

$$\frac{\lambda_0^4 e^{-\lambda_0}}{n(n-1)(n-2)}. \quad (10)$$

Five islands are generated and the four islands are located without gaps on the segment. The remaining island is located far from the four islands. The probability is given by

$$\frac{(n-5)\lambda_0^5 e^{-\lambda_0}}{n(n-1)(n-2)(n-3)}. \quad (11)$$

As the probability that other cases take place is very small, we can ignore them. Finally, the probability that four islands are aligned without gaps on the segment is given by the sum of Eqs. (10) and (11).

3. SEGMENT DISTRIBUTION

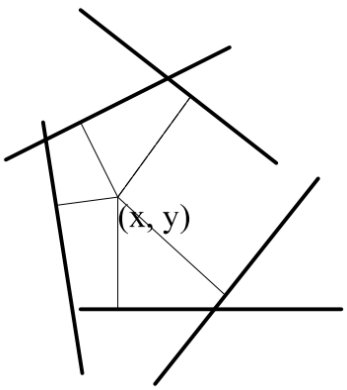

Figure 4. Distance from the point (x, y) to the segments. The bold line shows a segment and thin line shows one normal to the segment.

If a segment is approximately expressed as a straight line, we can define the distance from an arbitrary point (x, y) to the segment as shown in Fig. 4.

Let r_m be the minimum distance. If we draw a circle in the center point of (x, y) with a radius r, the probability that the circle crosses the segment is given by

$$P(r_m \leq r) = 1 - F(r) = \int_0^r p(r_m)\, dr_m, \quad (12)$$

where F(r) is the probability that the circle does not cross the segment and $p(r_m)$ is the probability density function of r_m. Eq. (12) leads

$$p(r) = -\frac{dF(r)}{dr}. \quad (13)$$

Hence, p (r) is related to the limiting radius of the island that means the radius beyond which the island cannot grow owing to the state of being tangent. The average density ρ of the segment is defined as N_s/S where N_s is the number of the segment within an area S. If the segment length *l* approaches zero, using the Poisson probability we can instantly derive F(r) as follows,

$$F(r) = \frac{(\rho S)^0 e^{-\rho S}}{0!} = e^{-\rho S}. \quad (14)$$

Some segments outside the circle may cross the circle.

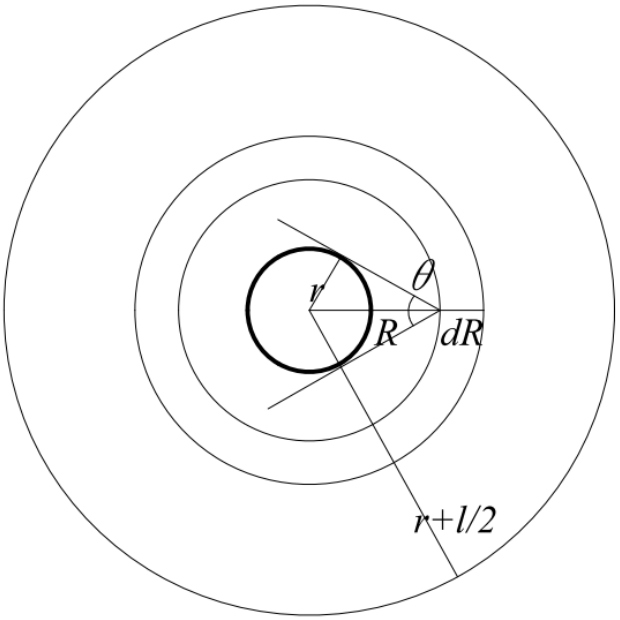

Figure 5. Geometric figure to calculate the number of segment that exists in a range from r to r+*l*/2. Only the segment within an angle of θ crosses the circle r.

Hence, we extend the number of the segment in the circle to that of the segment that lies outside the circle but cross the circumference. As shown in Fig. 5, the number of the segment that locates outside the circle, but crosses the circumference is given by

$$dN_{out} = \frac{\theta}{\pi}\rho 2\pi R dR = 4\rho sin^{-1}\left(\frac{r}{R}\right) dR, \quad (15)$$

where $\theta = 2sin^{-1}\left(\frac{r}{R}\right)$.

Setting s=r/R, we integrate Eq. (15) with an interval $\left[1, r/\left(r+\frac{l}{2}\right)\right]$,

$$N_{out} = 4\rho r^2 \int_1^{\frac{r}{r+\frac{l}{2}}} s^{-3} sin^{-1}(s) ds. \quad (16)$$

Using a partial integral, Eq. (16) becomes

$$N_{out} = 4\rho r^2 \left[-\frac{\pi}{4} + \left\{\frac{sin^{-1}(t^{-1})}{2t^2} + \frac{\sqrt{t^2-1}}{2}\right\}\right], \quad (17)$$

where $t = 1 + \frac{l}{2r}$.

Hence, we obtain the total number of the segment N,

$$N = \rho\pi r^2 + N_{out} = 2\rho r^2 \left[\frac{sin^{-1}(t^{-1})}{t^2} + \sqrt{t^2-1}\right]. \quad (18)$$

In electrodeposition, we assume *l*>>r that indicates that the copper islands growing on adjacent segments make contact. Hence, the limiting radius of the copper island beyond which the copper island cannot grow exists. Under *l*>>r, Eq. (18) approaches

$$N = \rho\left[\left(r+\frac{l}{4}\right)^2 - \left(\frac{l}{4}\right)^2\right]. \quad (19)$$

Substituting $N = \rho S = Eq.(19)$ into Eq. (14) and differentiating the result with respect to r, we have

$$p(r) = 4\rho\left(r+\frac{l}{4}\right) e^{2\rho\left(\frac{l}{4}\right)^2} \rho e^{-2\rho\left(r+\frac{l}{4}\right)^2}. \quad (20)$$

This is a Rayleigh distribution in two-dimensions [18]. Eq. (20) approximately has an expected value that is written as

$$r + \frac{l}{4} \approx \frac{1}{2\sqrt{2}} \sqrt{\frac{\pi}{\rho}} e^{2\rho\left(\frac{l}{4}\right)^2}. \quad (21)$$

The expected value is considered to be almost equal to the limiting radius of the island.

4. EXPERIMENTAL SET UP

The experimental procedure was as follows; An ITO glass (sheet resistance 6 Ω) of 1.5x1.0 cm^2 and a carbon plate of 3x4cm^2 were prepared for a cathode and anode electrode.

The cathode and anode electrode were put in an electrochemical bath including (mol L^{-1}): $CuSO_4 \cdot 5H_2O$, 3.1 and $KNaC_4H_4O_6 \cdot 4H_2O$, 2.1. The solution was strained using a membrane with a pore size of 0.17 μm to remove particles of Copper (II) hydroxide. The solution was maintained at a temperature of 313 K.

The rectangular pulse current having a current density of 22.4 mA cm^{-2} at a frequency of 500 Hz were provided in electrodeposition with a power supply. After electrodeposition in a time range from 5 to 180 s, the ITO glass on which copper electrodeposits were generated was rinsed with distilled water and dried.

The current efficiency was almost equal to 100 % in direct current electrodeposition.

The copper electrodeposit on the ITO glass was investigated to determine the number of islands using a Scanning Electron Microscope (SEM).

5. EXPERIMENTAL RESULTS AND DISCUSSION

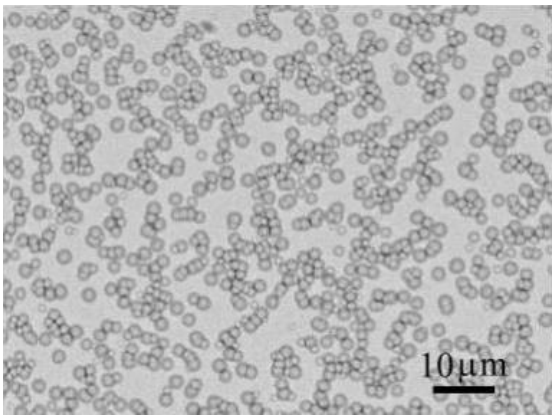

Figure 6. Typical SEM image of copper islands generated on the ITO glass at a growth time of 35 s. A great number of copper islands appear to be aligned on a little curved line.

As mentioned in the Introduction, this study aims to make clear the characteristic of the ITO surface as a nucleation site using the finite length segment model. Hence, in the experience first, the number of islands should be precisely counted, secondly, no overlap is needed to take place. This study is also different from the usual experiment of nucleation in which the electrochemical parameters are determined from the potentiostatic transient behavior [19-24].

Copper electrodeposition using a solution of potassium sodium tartrate is novel as far as we know. However, this study demonstrates not the nucleation behavior dependent on the electrochemical conditions but the characterization of the ITO glass surface. We will report the electrochemical kinetics and the copper thin film electrodeposited from the solution elsewhere.

Figure 6 shows a typical SEM image of copper islands grown on the ITO glass at a growth time of 35 s. The copper islands appear to align on a little curved line. For example, two, three, four, five, six and seven copper islands are observed to locate without gaps. In order to describe the array of copper islands, we introduce the fix length segment on which copper islands are generated.

5.1 The number of islands at a deposition time of 5 s

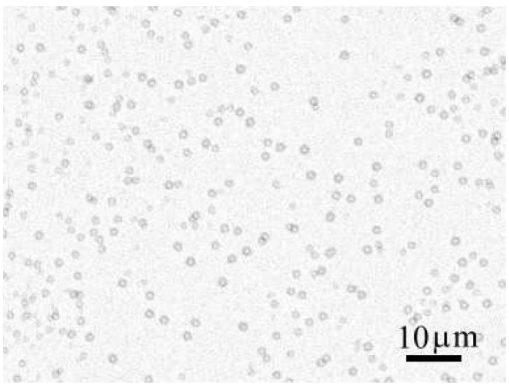

Figure 7. SEM image of copper islands generated on the ITO glass at a growth time of 5 s.

Figure 7 shows a SEM image of copper islands grown on the ITO glass at a growth time of 5 s. The observed full quantities of two, three, and four copper islands locating without gaps are listed in Table 1. In addition, substituting λ_0=1.15 and n=7 into the analytical result of the probability, we have the expected full quantities of the two, three, and four copper islands, which are also listed in Table 1.

Table 1. Comparison between the observed number of the two, three and four copper islands aligning without gaps and the expected values of them. The observed full quantity is obtained from the SEM image of copper islands generated at a growth time of 5 s. The expected full quantity is calculated using λ_0=1.15 and n=7.

variables	copper islands aligned without gaps		
	2	3	4
observed full quantity	43	8	2
expected full quantity	42.2	7	2.2

The total number of copper islands in Fig. 7 is 347. Hence, the number of the segments becomes 302. The expected full quantities are almost in good agreement with the observed ones.

To elucidate a difference in the characteristic of the surface as a nucleation site between the ITO glass in this study and Hopg in Reference 15, we calculate the values of λ_0 and n using AFM images (Fig. 6 (a) and (c) in Reference 15). The number of two islands aligning without a gap is 4 and 2 for the AFM grade Hopg and SPI-3 grade Hopg (the notation referenced in the Reference 15). We have λ_0= 0.54 and N_s=219 (8.54×10^{-3} $(\mu m)^{-2}$) for the AFM grade Hopg, and λ_0= 0.39 and N_s=279 (1.09×10^{-2} $(\mu m)^{-2}$) for SPI-3 grade Hopg when n=7. This indicates that the AFM grade Hopg has fewer nucleation sites than the SPI-3 grade Hopg. In addition, as the number of fix length segment in the ITO glass is 6.43×10^{-2} $(\mu m)^{-2}$, the ITO glass has more nucleation sites. Thus, the characterization of the surface as a nucleation site is demonstrated.

5.2 The number of islands at a deposition time of 10 s

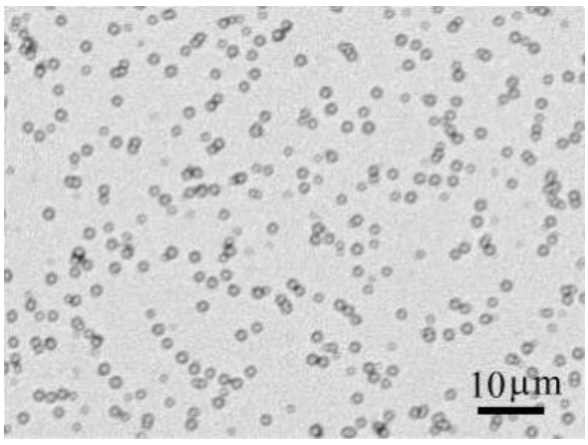

Figure 8. SEM image of copper islands generated on the ITO glass at a growth time of 10 s.

Figure 8 shows a SEM image of copper islands grown on the ITO glass at a growth time of 10 s. Treating the number of the copper islands at a growth time of 5 s as an initial condition, we make an attempt to estimate an increase in the number of islands locating without gaps at 10 s.

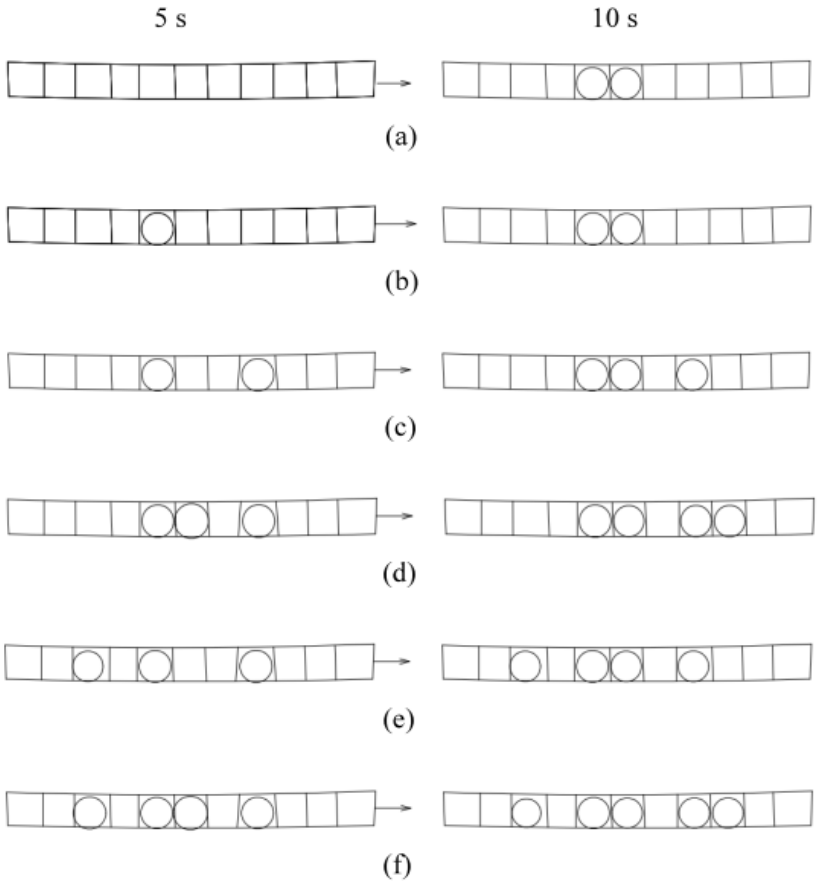

Figure 9. Examples that the number of the two islands aligned without a gap at a growth time of 10 s increases in comparison with that at a growth time of 5 s .

The cases that increase the number of the two islands locating without a gap are shown in Fig. 9. Other cases are neglected because their probabilities are too small.

The probability for the increase in the two islands located in adjacent site is given by the summation of the cases in Fig. 9 (for n=7),

$$P_2^+ = e^{-\lambda_0}\frac{{\lambda_1}^2 e^{-\lambda_1}}{n} + \lambda_0 e^{-\lambda_0}\frac{2\lambda_1 e^{-\lambda_1}}{n} + \lambda_0^2 e^{-\lambda_0}\frac{2(n-3)\lambda_1 e^{-\lambda_1}}{n(n-1)} + e^{-\lambda_0}\frac{n-3}{n(n-1)}\lambda_1^3 e^{-\lambda_1}$$
$$+e^{-\lambda_0}\frac{(n-4)(n-5)}{n(n-1)(n-2)}\lambda_1^4 e^{-\lambda_1} + \lambda_0^3 e^{-\lambda_0}\frac{6(3n-17)}{n(n-1)(n-2)(n-3)}\lambda_1 e^{-\lambda_1}, \quad (22)$$

where $\lambda_1 = [N_i(t = 10\ s) - N_i(t = 5\ s)]/N_s$.

In a similar way, the probability for the decrease in the two islands located in an adjacent site is given by

$$P_2^- = \lambda_0^2 e^{-\lambda_0}\frac{2\lambda_1 e^{-\lambda_1}}{n(n-2)} + \lambda_0^2 e^{-\lambda_0}\frac{\lambda_1^2 e^{-\lambda_1}}{n(n-1)} + \lambda_0^3 e^{-\lambda_0}\frac{2(n-4)\lambda_1 e^{-\lambda_1}}{n(n-1)(n-3)}. \quad (23)$$

The first term on the right-hand side in Eq. (23) indicates the probability that one island is generated at an adjacent site of the two islands aligned without a gap. The second term on the right-hand side in Eq. (23) indicates the probability that the two islands are generated and one is at least located at an adjacent site of the two islands aligned without a gap. The third term on the right-hand side in Eq. (23) indicates the probability that on the segment on which two islands are present without a gap and one island is apart from the two islands, one island is generated at an adjacent site of the two islands. Thus, the net probability for the increase in the two islands located in an adjacent site is given by

$$\Delta P_2 = P_2^+ - P_2^-. \quad (24)$$

In a similar way, the probabilities for the increase in the three and four islands locating without gaps are given by,

$$\Delta P_3 = e^{-\lambda_0}\frac{\lambda_1^3 e^{-\lambda_1}}{n(n-1)} + \lambda_0^2 e^{-\lambda_0}\frac{(4n-10)\lambda_1 e^{-\lambda_1}}{n(n-1)(n-2)} + \lambda_0 e^{-\lambda_0}\frac{(5n-14)\lambda_1^2 e^{-\lambda_1}}{n(n-1)} - \lambda_0^3 e^{-\lambda_0}\frac{2(n-3)\lambda_1 e^{-\lambda_1}}{n(n-1)(n-2)(n-4)}, \quad (25)$$

and

$$\Delta P_4 = e^{-\lambda_0}\frac{\lambda_1^4 e^{-\lambda_1}}{n(n-1)(n-2)} + \lambda_0 e^{-\lambda_0}\frac{24\lambda_1^3 e^{-\lambda_1}}{(n-1)^2(n-2)} + \lambda_0^2 e^{-\lambda_0}\frac{3\lambda_1^2 e^{-\lambda_1}}{n(n-1)} + \lambda_0^3 e^{-\lambda_0}\frac{2\lambda_1 e^{-\lambda_1}}{n(n-1)(n-2)} - \lambda_0^4 e^{-\lambda_0}\frac{2\lambda_1 e^{-\lambda_1}}{n(n-1)(n-2)(n-3)}. \quad (26)$$

In comparison with the two, three, and four copper islands aligning without gaps at a growth time of 5 s, increases in those at a growth time of 10 s are listed in Table 2.

Table 2. An increase in the two, three, and four copper islands aligning without gaps at a growth time of 10 s in comparison with those at a growth time of 5 s. The expected increment is calculated using λ_0=1.15 and n=7.

variables	copper islands aligned without gaps		
	2	3	4
observed full quantity	45	10	2
observed ΔP_i (i=2,3,4)	2	1	0
Expected ΔP_i (i=2,3,4)	1.4	0.6	0.07

The expected increment quantities are almost in good agreement with the observed ones. However, the coalescence of copper islands is observed at a growth time of 15 s. It is difficult to count the number of the two, three, and four islands precisely. Hence, the probability analysis in this study is appropriate to the probability analysis of the generation of the island in electrodeposition at the early stage.

5.3 The limiting radius of copper islands

In the Section 5.1, the values of λ_0, n, and N_s were determined as 1.15, 7, and 302 respectively. Using the dimensions of the SEM image in Fig. 6, we have $\rho=6.43x10^{-2}$ $(\mu m)^{-2}$. In addition, as the total number of copper islands in Fig. 8 is 405, the value of λ_1 becomes 0.192. Using these values, r and *l* that satisfy Eq. (21) become r=1.8 μm and *l*=6.0 μm.

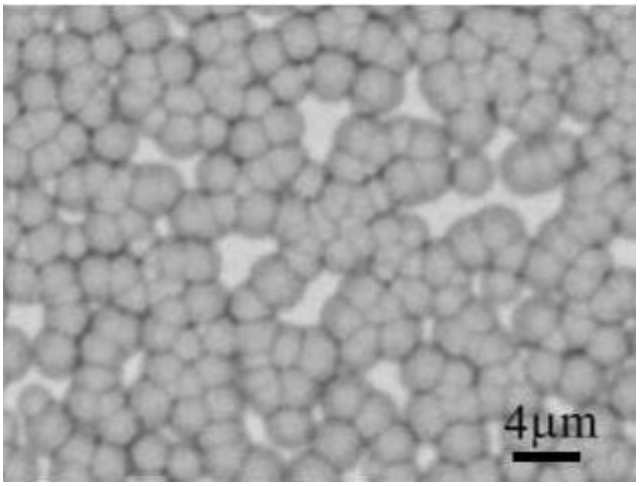

Figure 10. SEM image of copper islands generated on the ITO glass at a growth time of 180 s.

Figure 10 shows a SEM image of copper islands at a growth time of 180 s. The copper islands make contact with each other. The average radius of the island in Fig. 10 is approximately 1.6 μm. The expected value r is consistent with the experimental value. However, the expected length of the segment *l* seems to be shorter than that in Figs. 6 and 7.

6. CONCLUSIONS

The fixed length segment model is proposed to describe the islands aligned without gaps and distribution of the segment. The probabilities for the generation of the two, three, and four islands locating without gaps on the segment are analytically derived. In addition, the fixed length segment distribution derived analytically yields the limiting radius of the island beyond which the island cannot grow. In comparison with the copper electrodeposition on the ITO glass, the fixed length segment model well explains the distribution of the copper islands and the limiting radius of the copper island, and enables the characterization of the surface of the ITO glass as nucleation sites.

ACKNOWLEDGEMENTS
The author deeply appreciates Miss H. Hanawa for their help in the experimental setup.

References

1. A. Mashreghi and H. Zare, *Curr. Appl. Phys.*, 16 (2016) 599.
2. Y-R. Kim, S. C. S. Lai, G. Zhang, D. Perry, T. S. Miller, and P. R. Unwin, *J. Phys. Chem. C*, 119 (2015) 17389.
3. B. Im and S. Kim, *Electrocim. Acta*, 130 (2014) 52.
4. J. Ustarroz, J. Hammons, T. Altantzis, A. Hubin, S. Bals, and H. Terryn, *J. Am. Chem. Soc.*, 135 (2013) 11550.
5. U. Reuter, *J. Electroanal. Chem.*, 136 (1992) 167.
6. B. Scharifker and G. Hills, *Electrochim. Acta*, 28 (1983) 879.
7. H. Brune, *Surf. Sci. Rep.*, 31 (1998) 121.
8. J. W. Evans, P. A. Thiel, and M. C. Bartelt, *Surf. Sci. Rep.*, 61 (2006) 1.
9. N. Eliaz and M. Eliyahu, *J. Biomed. Mater. Res. A.*, 80 (2007) 621.
10. K. Sangwal, *Scientometrics*, 92 (2012) 575.
11. E. G-García, M. R-Romo, M. T. R-Silva, and M. P-Pardavé, *Int. J. Electrochem. Sci.*, 7 (2012) 3102.
12. M. Avrami, *J. Chem. Phys.*, 7 (1939) 1103.
13. M. Avrami, *J. Chem. Phys.*, 8 (1940) 212.
14. D. Grujicic and B. Pesic, *Electrochim. Acta*, 47 (2002) 901.
15. S. C. S. Lai, R. A. Lazenby, P. M. Kirkman, and P. R. Uhwin, *Chem. Sci.*, 6 (2015) 1126.
16. M. Huynh, D. K. Bediako, Y. Liu, and D. G. Nocera, *J. Phys. Chem. C*, 118 (2014) 17142.
17. *S. M. A Hossain* and *M. Saitou*, *Open Electrochem. J.*, 4 (2012) 9.
18. C. Metzen, P. Krauss, and B. Fabry, *Arxiv* (2011).
19. A. Milchev and I. Krastev, *Electrochim. Acta*, 56 (2011) 2399.
20. A. Mashreghi and H. Zare, *Curr. Appl. Phys.*, 16 (2016) 599.
21. Y. Zhao, F. X. Deng, L. F. Hu, Y. Q. Liu, and G. B. Pan, *Electrochim. Acta*, 130 (2014) 537.
22. I. Danaee, *J. Ind. Eng. Chem.*, 19 (2012) 1008.
23. A. H. Sulayman, S. A. M. Mohammd, A. H. Abbar, *Int. J. Electrochem. Sci.*, 9 (2014) 6328.
24. G. C. Arteaga, M. A. del Valle, M. Antilen, M. Romero, A. Ramos, L..Hernandez, M. C. Arevalo, E. Patror, and G. Louarn, *Int. J. Electrochem. Soc.*, 8 (2013) 4120.